J. Ind. Geophys. Union (July 2015)
v.19, no.3, pp:312-321

Assessment of Snowmelt Runoff in the Eastern Himalayan Region under Climate Change Scenarios

A. Bandyopadhyay, A. Bhadra, N. Chiphang*, K.T. Senzeba

Department of Agricultural Engineering, North Eastern Regional Institute of Science and Technology, Nirjuli (Itanagar), Arunachal Pradesh 791109, India.

*Corresponding Author : ecks.wove@gmail.com

ABSTRACT

In Eastern Himalayan region, snow melt is the major source of fresh water. Also, snow covered areas lying at low altitudes are expected to be most vulnerable to global warming. Thus, assessment of the snowmelt runoff under different climatic scenarios is important for efficient management and planning of water resources, which can be used towards mitigating the influence of climate change. Eastern Himalayan region of India with its unique topography and inaccessibility is lagging behind in the studies related to snow and glacier melt modelling and impact of climate change to water resources. Nuranang river catchment of Tawang River basin located in Tawang district of Arunachal Pradesh was selected as the study area for the present study. Average snow accumulation and depletion patterns of the basin showed a smaller peak in terms of snow cover area percentage (SCA%) in the month of November and a larger one in April. A Windows-based semi-distributed deterministic model was used in this study to predict the snowmelt runoff using degree-day approach , which requires SCA% for different elevation zones as input. The model was calibrated for depletion periods of 2006, 2007, and 2009 and validated for year 2004 satisfactorily. Further, the projected temperature and precipitation data downloaded from NCAR's GIS data portal for different emission scenarios (SRES), viz., A1B, A2, B1; and IPCC commitment (non-SRES) scenario for different future years (2020, 2030, 2040 and 2050) were used to generate snow depletion curves for future and compared with conventional depletion curve for present climatic condition. The same were used to evaluate the future stream flow under different projected climatic scenarios. Evaluation of the impact of climate change showed that change in cumulative snowmelt depth and snow depletion for different future years is highest under A1B and lowest under IPCC Commitment scenarios, whereas A2 and B1 values are in-between A1B and IPCC Commitment.

INTRODUCTION

Glacier and snow at high mountain peaks are the ultimate resources for fresh water. For planning and assessment of water resources in mountain basins, mathematical modelling and mapping of glacier and snow melting plays a vital role. Bates et al. (2008) reported that Snow Cover Area (SCA) has been significantly decreasing in Northern Hemisphere and the global surface temperature has been increasing in the range of 0.56–0.92 °C between 1906 and 2005, with a more rapid warming trend over the last 50 years. The increase in global average temperature since the mid-20th century is very likely due to the increase in anthropogenic Green House Gases (GHGs) concentration (Pachauri and Reisinger, 2007). The trends of warming temperature have significant impact on glaciers and snow cover regions around the world. On the other hand, with ever increasing population, more demands for water from irrigation, domestic, and industrial sectors are imposing direct impact on hydrologic cycle of the earth. Monitoring and estimation of snowmelt runoff becomes essential for supporting, planning, and management of water resources.

The major impact of climate change in the Indian sub-continent would be on the hydrology and water resources. In India, the effects of global warming can be witnessed on snow covered mountain peaks of Himalayan region. The areas covered by snow at low altitude are expected to be most vulnerable to global warming. The major river systems of the Indian sub-continent, Ganga, Brahmaputra, and Indus, which originate from the Himalayas, are expected to be vulnerable to the climate change because of substantial contribution from snow and glaciers (Singh and Jain, 2002; Singh and Kumar, 1997). Many significant advances in remote sensing and Geographic Information System (GIS) technologies made it possible to monitor more precisely and map more accurately the extent of snow cover area. Use of Normalized Difference Snow Index (NDSI) has simplified the determination of SCA% in a basin. Snow Cover Depletion Curve (SDC) is one of the major inputs to various snowmelt runoff models, which support snowmelt runoff simulation. For most of the snow-fed or glacier-fed river basins at high altitude, a reliable mathematical model with strong snow and glacier melt simulation capability, which can handle poorly gauged catchments with limited data, is very much essential. Singh and Singh (2001) reported that either an energy balance approach or a temperature index (degree-day) approach may be used to simulate the snowmelt runoff. Energy balance snowmelt models require extensive data that are not easily available in most of snow/ice covered area of Himalayan

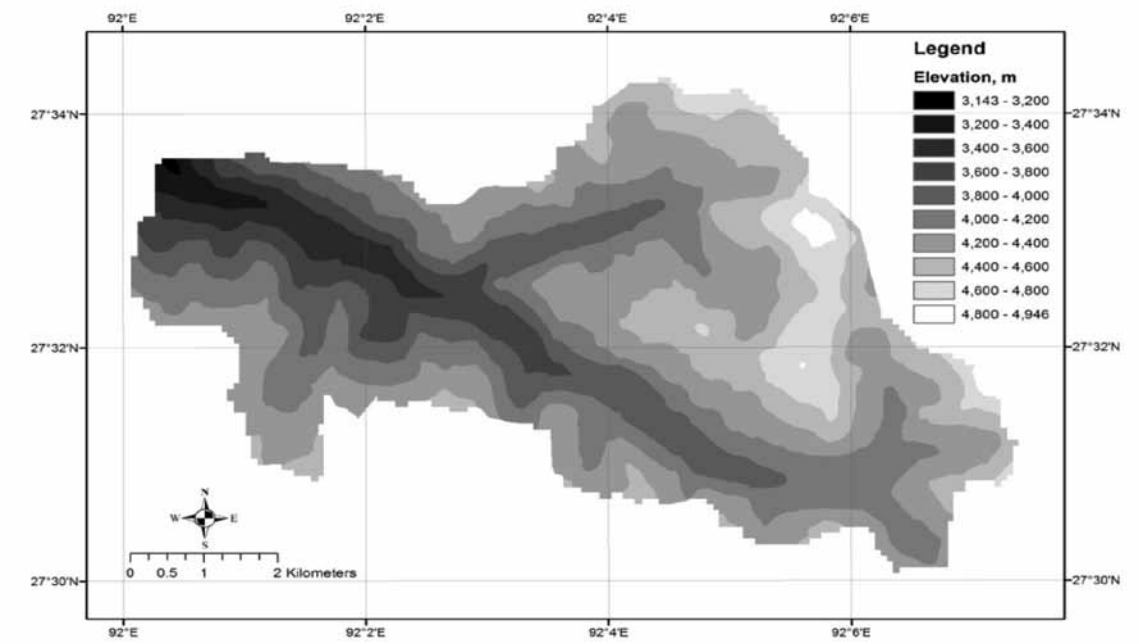

Figure 1. Nuranang river basin in Tawang district of Arunachal Pradesh, India.

region. On the other hand, the temperature index used a degree-day factor, which is a proportionality coefficient that can compute melt rates based on air temperature alone.

In the present study, an attempt is made to simulate the snowmelt and evaluate the change in snow cover depletion and corresponding streamflow under different projected climatic scenarios using SRM (Martinec et al., 2008) in a snow covered river basin of eastern Himalaya in Arunachal Pradesh, India. Arunachal Pradesh is a state in northeast India that has glaciers and good seasonal snow cover at higher elevation range, which is inaccessible and has minimal meteorological network. Topography of the region is tortuous mountain system with varying elevation, providing a huge potential for generating hydro-power. Eastern Himalayan region of India is lacking studies related to snow and glacier melt modelling and impact of climate change on water resources. Studies on depletion of SCA, estimation of water melt from snow and glaciers, and prediction of snowmelt runoff under changed climate are becoming crucial in this region. Such study is much needed for informed and efficient planning and management of water resources including flood forecasting, reservoir operation and design of hydraulic structures.

Keeping the above mentioned facts in view, the present study has been taken up to calibrate and validate a hydrological snowmelt model, using observed climatic inputs and streamflow. This is followed by detailed estimation of the effect of warmer climate on the acceleration of depletion of SCA. Finally, we have carried out a study on potential impacts of projected climate warming on snowmelt runoff.

METHODOLOGY

Study area and acquisition of data

Nuranang river basin (Figure 1) located at Tawang district of Arunachal Pradesh, India with an area of 52 km^2 was selected for the present study. Nuranang river, a tributary to Tawang River, originates from Sela Lake and joins Tawang River as Nuranang fall at Jang. The altitude of the Sela Lake is 4211 m above MSL and it lies at 27° 30' 09" N and 92° 06' 17" E. The CWC discharge site at Jang is selected as the outlet point and it lies at 27° 33' 01" N and 92° 01' 13" E, with an elevation of 3474 m above MSL. Elevation of the basin ranges from 3143 m to 4946 m above MSL ,with an average slope of 51%. Latitude ranges from 27° 30' N to 27° 35' N, whereas longitude is in between 92° E to 92° 7' E. The entire river basin is dominated by seasonal snow.

Automatic Weather Station (AWS) and Snow Water Equivalent Recorder (SWER) are installed at Sela Top inside the Indian Military Based Camp (Communication DET) near the Sela Lake, Tawang district in Arunachal Pradesh, India. The meteorological and hydrological data from 2000–10 were collected from CWC office, Itanagar, Arunachal Pradesh, India. Satellite images (LISS-III/AWiFS) for the five block years (2005–06, 2006–07, 2008–09, 2009–10, and 2010–11) of snow accumulation and depletion period (October–May) were procured from NRSC, ISRO, Hyderabad, India. SRTM with resolution 90 m × 90 m Digital Elevation Model (DEM) was downloaded for the study area from http://gisdatadepot.com/dem. For this

study, projected temperature and precipitation data were downloaded as shapefiles with regular grid points from NCAR's GIS Program Climate Change Scenarios GIS data portal (https://gisclimatechange.ucar.edu/) for different emission scenarios (SRES; Girod et al., 2009; Nakicenovic *et al*., 2003), viz., A1B, A2, B1; and IPCC commitment scenario (non-SRES) for different future years (2020, 2030, 2040, and 2050) (CCSM3; Collins et al., 2006). The projected temperature and precipitation data at CWC Jang site were obtained by spatially interpolating the gridded data using Inverse Distance Weighting (IDW). This was followed by statistical downscaling using linear regression models developed between past 10 years (2000–10).In this exercise Community Climate System Model (CCSM) data and observed data at CWC Jang (Swain et al., 2014) were made use of.

Generation of hypsometric curve and SCA percentages

The total elevation of the study site ranges from 3143 m to 4964 m. The SRM model is sensitive to lapse rate. As CWC station is located at low elevation (3474 m), lapse rate was used to adjust mean daily temperature at hypsometric mean elevation (4215 m). Area elevation curves or hypsometric curve for the whole basin was derived from DEM using ArcGIS 10. SCA% is referred as the areal extent of snow covered ground, which is usually expressed as percentage of total area in a given region. The SCA% can be estimated using GIS software: Earth Resources Data Analysis System (ERDAS) and ArcGIS. In Himalayas, cloud cover is quite common. In the visible portion of the electromagnetic spectrum, snow and cloud both appear bright white and create confusion in SCA estimation. Mountain shadow also makes it difficult for discrimination of SCA under mountain shadow from snow free areas. The NDSI is useful for the identification of snow as well as for separating snow from clouds. It uses the high and low reflectance of snow in visible (Green) and SWIR bands, respectively and it can also delineate and map the snow in mountain shadows (Kulkarni et al., 2002). In the present study, a NDSI model was coded in ERDAS for discrimination of snow from the satellite imagery data for the study area. The model was based on Kulkarni et al., (2006).

Model setup

Windows-based snowmelt runoff model WinSRM (Martinec et al., 2008) was used in this study. The main characteristic of the SRM model is that it can be used effectively in mountain region with limited data availability and it is relatively simple. The SRM model also successfully underwent tests by the WMO in regard to runoff simulations (WMO, 1986) and to partially simulated conditions of real time runoff forecasts (WMO, 1992). The model requires three basic daily values of the input variables, viz., temperature, precipitation, and SCA%. The average daily temperature was used to compute the daily number of degree-days responsible for snowmelt. Precipitation on daily basis was collected from CWC observation site at Jang. Multi-spectral satellite images (LISS-III/AWiFS) were used to determine the SCA%. Daily SCA% was determined by interpolating periodical snow cover percentages as obtained from procured monthly images. Seven parameters were involved to run the SRM model, viz., runoff coefficients, degree-day factor, temperature lapse rate, critical temperature, rainfall contribution area, recession coefficient and time lag.

Determination of model parameters

Among seven parameters, three parameters (degree-day factor, temperature lapse rate and recession coefficient) were determined. The degree-day factor converts the number of degree-days into the daily snowmelt depth. It is daily decrease in snow water equivalent per degree increase in degree-days (Martinec, 1960). To obtain daily SWE, SWER was installed at Sela Top. For one snow accumulation and ablation period of the Nuranang basin, average degree-day factor was obtained as 0.3 cm/°C. This average value matches quite well with the average of recommended monthly values (WMO, 1964). Different values for different ablation months were used as per WMO recommendation (WMO, 1964). Temperature variation is major factor for melting of snow/ice at high mountain peaks, so lapse rate is an important parameter in hydrological model , such as SRM to determine the temperature variation with elevation. The temperature lapse rate is used to adjust temperature measured at the basin reference elevation to each zone's hypsometric mean elevation. For the present study, the temperature lapse rate was estimated by simple linear regression for maximum, minimum and mean monthly temperatures with altitudes. Hourly temperature data of 18 AWS stations of Arunachal Pradesh for the period of five years (2008–2012) were downloaded from MOSDAC (http://www.mosdac.gov.in/). From linear regression results, an average value of 0.5 °C/100 m as lapse rate for mean air temperature was considered for the model simulation (Bandyopadhyay et al., 2014). The linear regression model was validated for Sela top station from the period of November 2012 to April 2013 by comparing the temperatures computed by the model and temperature measured by AWS at the station. The r^2 for mean temperature was 0.81. The results show that the performance of the regression models are satisfactory and can be adopted for Arunachal Himalaya. The historical discharge values of Nuranang river, Q_n (average daily discharge on n^{th} day) and Q_{n+1} (average daily discharge on

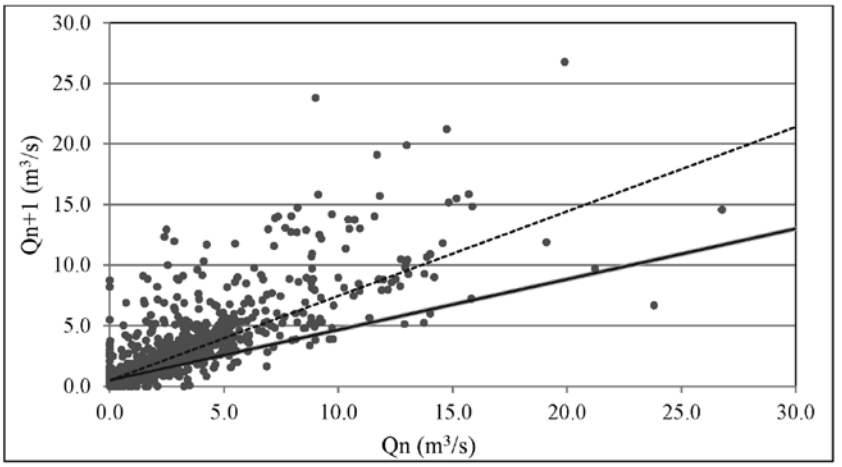

Figure 2. Recession flow plot Qn vs. Qn+1 for the Nuranang basin.

n+1th day) were plotted against each other and the lower envelope line of all points was considered to indicate the *k*-values (Figure 2). The constants *x* and *y* were obtained as 0.61 and 0.104 respectively.

Calibration of model

Other required parameters like runoff coefficients, critical temperature, rainfall contribution area, and time lag were calibrated. The runoff coefficient is different for snow and rain. The calibration ranges of runoff coefficients for snow and rain were taken as 0.1 to 1.0 (Martinec et al., 2008). The critical temperature is a pre-selected value of temperature, which determines whether the precipitation event is rain or snow. Critical temperature was calibrated for the basin in the range of 0–4.0 °C for all calibration years. Rainfall contribution area helps to determine whether the rainfall induced runoff is added to snowmelt induced runoff only from the snow-free area or from the entire zone area. *RCA* equals to 0 or 1 or combination of 0 and 1 were tried in this study. Time lag indicates the time which the rising of discharge lags behind the rise of temperature. The study area having a small size basin and steep slope, a lag time of 2, 4, 6, 8, 10, and 12 hours were tried for calibration. Calibration of model was done for snow ablation period of three years viz., 2006, 2007, and 2009. On other side, validation of WinSRM was performed for the year 2004.

For the present study, baseflows were separated from the observed total streamflow using an algorithm described by Hughes et al. (2003) and Welderufael and Woyessa (2010) and direct runoff was used in the simulation. To evaluate the performance of WinSRM, predicted discharges were compared with the observed ones. Statistical tests can give the quantitative performance of the prediction. Here, two dimensionless statistical performance criteria viz., ME and CRM were used to evaluate the performance of the model. WinSRM model was calibrated using observed data for the Nuranang river basin.

Development of climate affected depletion curve for the selected hydrological year

Hydrological year 2007 was selected to study the effect of climate change under different projected scenarios on snow depletion curve. The temperature and precipitation data for the year 2007 were rectified to represent the present climatic condition by eliminating the impact of yearly fluctuation of temperature and precipitation on the snow cover depletion (Martinec et al., 2008). Monthly SCA% was obtained from periodical snow cover mapping for the selected hydrological year 2007. By interpolating monthly SCA%, Conventional Depletion Curve (CDC) for selected hydrological year was generated by plotting daily snow covered percentage with respect to corresponding days, which can be seen in Figure 6. Depletion curves indicate the snow coverage on each day of the melt season. They have also been used as indicator of snow reserves and water equivalent. But the decline of snow cover extent not only depends on the initial snow reserves, but also on the climatic conditions of the year being considered. The future course of the depletion curves of the snow coverage can be evaluated from the Modified Depletion Curve (MDC). These curves can be derived from the CDC. MDC relates the SCA to the cumulative snowmelt depths. These curves enable the snow coverage to be extrapolated manually by the user, several days ahead by temperature forecasts so that this input variable can be available for discharge forecasts. So, the MDC can be used to evaluate the snow reserves for seasonal runoff forecasts. In a warmer climate, this cumulative snowmelt depth will be reached at an earlier date and the CDC of the snow coverage will be shifted accordingly. Using these climate-affected conventional depletion curves together with precipitation and temperatures given by a

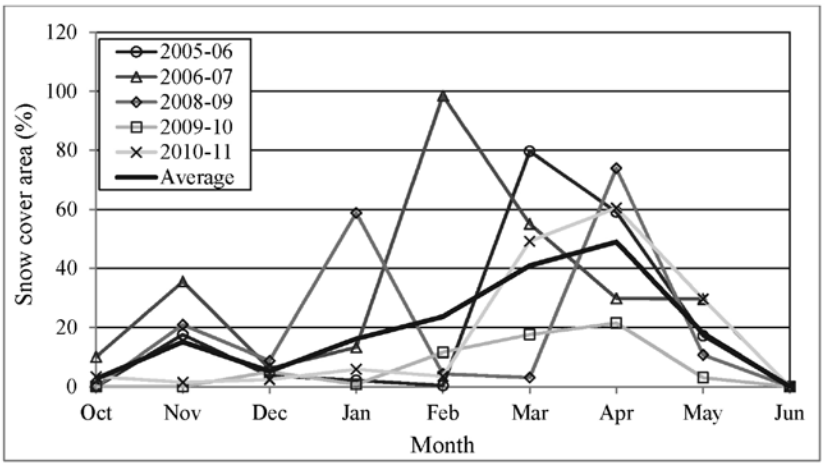

Figure 3. Snow accumulation and depletion pattern of Nuranang basin.

projected climate scenario, the future changed runoff can be computed. MDC_{INCL} was derived from CDC (Rango and Martinec, 1994). MDC_{INCL} indicates how much snow including new snow falling during the snowmelt season or period while a CDC indicates snow covered areas in the present time. MDC_{EXCL} was derived from MDC_{INCL} by eliminating melt depths referring to new snow from the accumulated snowmelt depth obtained by considering the effect of rectified temperature and precipitation for selected hydrological year. MDC_{CLIM} takes into account the amount of snowfall changed by the new climate. If there is no change, it is identical with MDC_{INCL}. CDC_{CLIM} was generated by plotting the daily value of SCA% against the shifted date of snow depletion due to changed climate. The curve indicates the change in duration of snow depletion period, its start and end time and change in the rate of depletion under projected climatic scenarios. The derived CDC_{CLIM} under different projected climatic scenarios (A1B, A2, B1, and IPCC Commitment) for different future years (2020, 2030, 2040, and 2050) (Figure 6) were used as model input along with changed temperature and precipitation to compute the climate-affected runoff.

RESULTS AND DISCUSSION

Variations of snow cover percentages during accumulation and ablation period (October–June) have been determined for all five block years (2005–06, 2006–07, 2008–09, 2009–10, and 2010–11) of the Nuranang river basin. From the observed long term monthly average temperature data, it was noticed that during winter season the temperature initially decreased in the month of November/December but then increased in the month of January. Again temperature decreased during February/March. Variations of SCA% for individual block years also follow this unique trend. It can be seen that in most of the block years, two peaks have been observed; the first peak is around November/December and the second peak around March/April, which is larger than the first one (Figure 3). Snow depletion curves for the selected calibration years (2006, 2007, and 2009) were generated using monthly SCA%. The daily SCA% was determined by interpolating the satellite image derived monthly SCA values. These SCA values on daily basis for depletion period were used as model input.

The model was calibrated for depletion period of 2006 (1st March–30th June), 2007 (15th February–15th June), and 2009 (12th April–30th June). For obtaining best possible combination of model calibration parameters, only one parameter at a time was varied within feasible range keeping other parameters fixed at their starting values. Depending on values of performance indicators ME and CRM on comparing predicted and observed runoff, best possible values of critical temperature (T_{CRIT}) were obtained as 2.0, 1.0, and 4.0 °C for the years 2006, 2007, and 2009, respectively. Since the area of Nuranang basin is very small, better ME and CRM were found using time lag (L) of 2 hours for all three calibration years. Better matches were obtained for runoff coefficient of snow (c_S) as 0.1, 0.1, and 0.6, and runoff coefficient of rain (c_R) as 0.6, 0.9, and 0.5 for the years 2006, 2007, and 2009, respectively. Better performance indicators were obtained for rainfall contribution area (RCA) as "mix (0 & 1)" for all calibration years. Considering the statistical results for individual calibration parameters, the best possible combinations of calibration parameters were determined for each calibration year. The calibration results are given in Table 1 and time series as well as scatter plots are shown in Figure 4. Model was simulated using best possible set of calibration parameters for each calibration year. Validation of WinSRM model was performed for the year 2004 (1st February–30th June) using average values of calibration parameters as determined for calibration years. From validation results, the ME and CRM were obtained as 0.66 and -0.04, respectively. The time series as well as

Table 1. Best parameter sets and calibration results

Parameter	2006	2007	2009	Average
*T*crit, °C	2	1	4	2.33
Lag Time (*L*), h	2	2	2	2
Snow Runoff Coefficient (c_S)	0.1	0.1	0.6	0.3
Rain Runoff Coefficient (c_R)	0.6	0.9	0.5	0.7
Rainfall Contributing Area (*RCA*)	Mix	Mix	Mix	Mix
ME	0.66	0.69	0.63	
CRM	-0.19	-0.08	0.05	

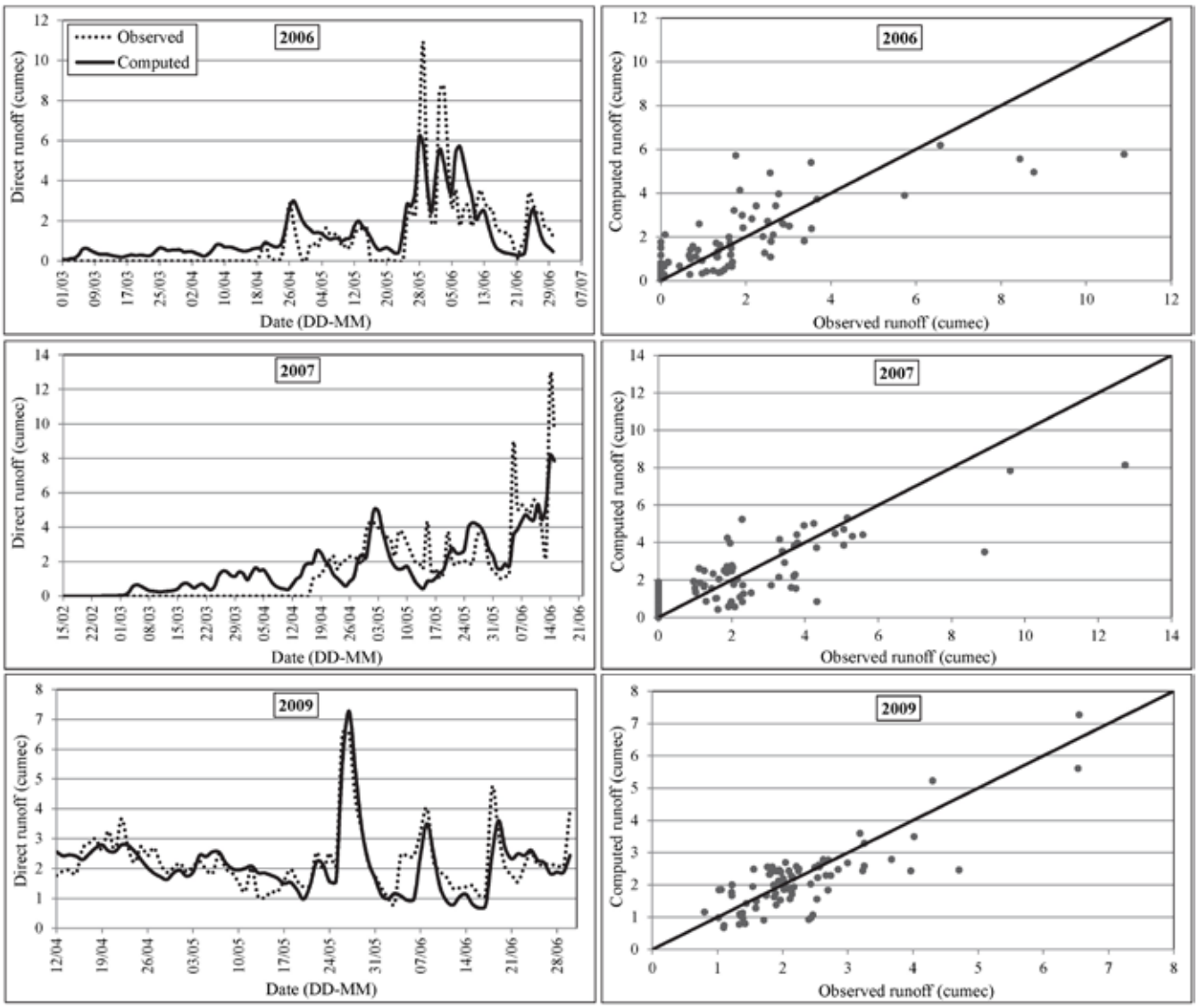

Figure 4. Time series and scatter plots for all three calibration years.

scatter plots for the validation year are shown in Figure 5. From the calibration and validation results, it can be said that under limited data availability condition; WinSRM is successfully calibrated for a representative river basin in eastern Himalayan region.

CDC for the selected hydrological year (2007) was generated. MDC_{CLIM} and CDC_{CLIM} were determined for future years (2020, 2030, 2040, and 2050) under projected scenarios. The shift of start and end dates of the snow cover depletion curves for different future years under

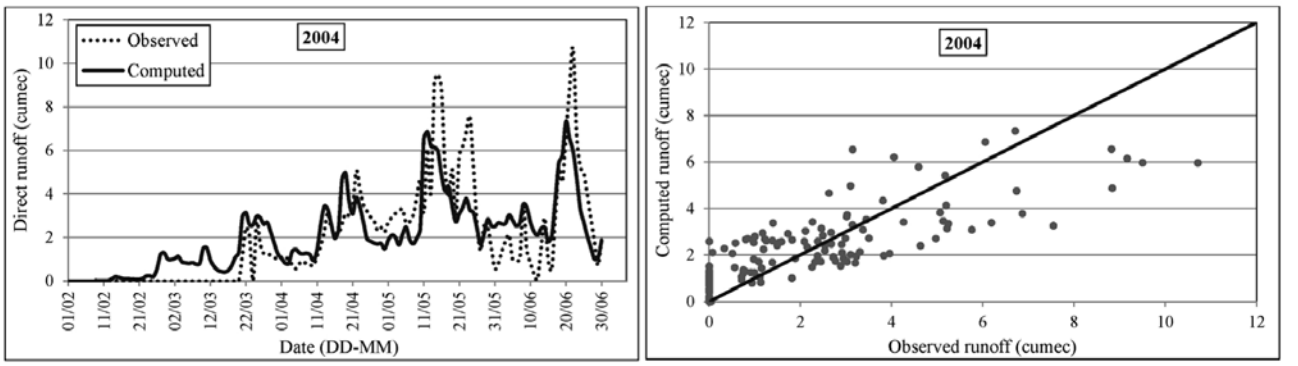

Figure 5. Time series and scatter plot for validation year 2004.

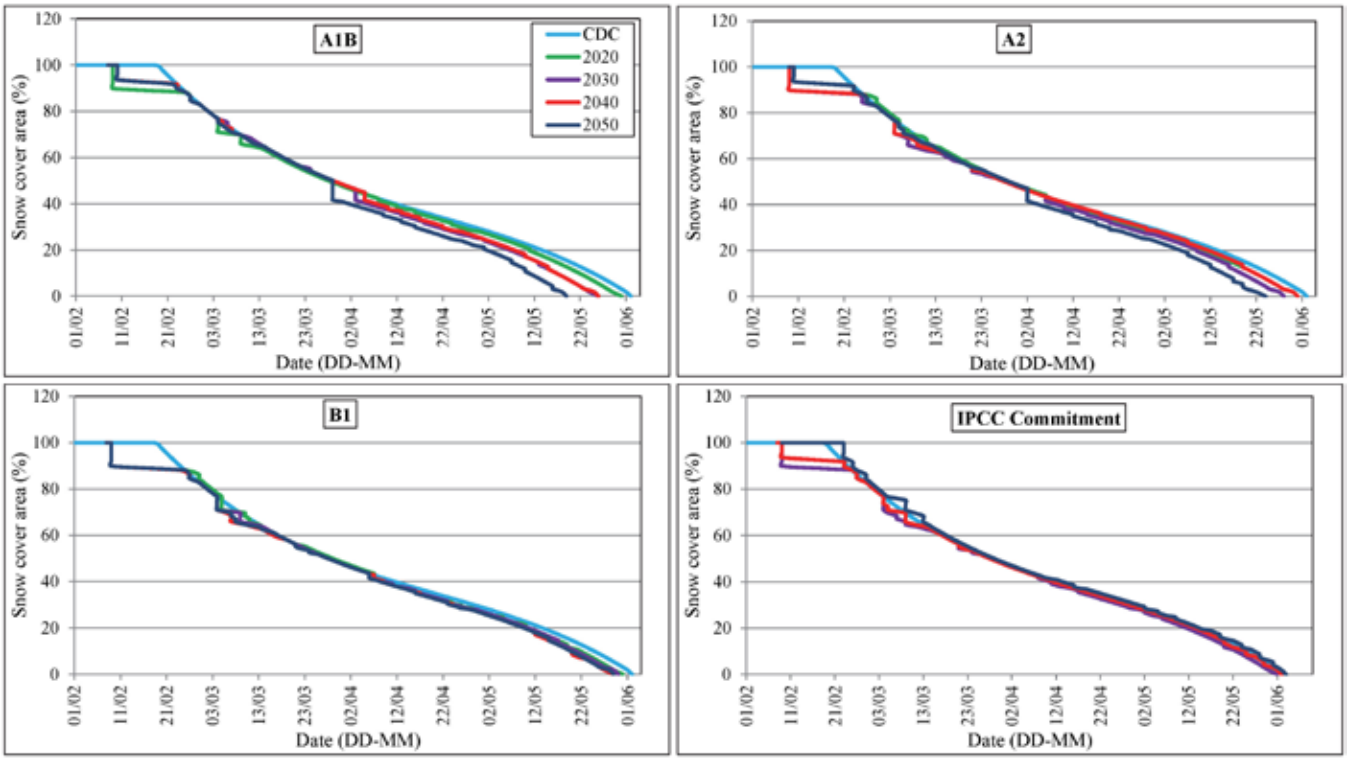

Figure 6. Climate affected depletion curves (CDCCLIM) for all projected scenarios.

projected climatic scenarios were compared to present climatic condition (Figure 6). Under A1B, the start date of depletion shifts back from 10 days in 2020 to nine days in 2050; the end date shifts back from two days in 2020 to 14 days in 2050; modifying the snowmelt period from 112 days in 2020 to 99 days in 2050. Under A2, the start date of depletion shifts back from 10 days in 2020 to nine days in 2050; the end date shifts back from two days in 2020 to nine days in 2050; modifying the duration of snowmelt period from 112 days in 2020 to 104 days in 2050. Under B1, the start date of depletion shifts back 10 days for all the future years; backward shifting of end date varies from two days in 2020 to four days in 2050; and the duration of snowmelt period varies from 112 days in 2020 to 110 days in 2050. Under IPCC Commitment, the start date of depletion shifts back 10 days in 2020 whereas shifts forward four days in 2050. Similarly, the end date also shifts back one day in 2020 but shifts forward by one day in 2050; resulting the duration of snowmelt period of 113 days in 2020 and 101 days in 2050. Backward shifts in end dates with change in temperature over future years under projected climatic scenarios were also compared. It was observed that if temperature increases, shift of end dates in the backward direction increases. For any future year, number of days of backward shift in end dates is highest under A1B and lowest under IPCC Commitment scenarios, respectively. Backward shifting of end dates under A2 and B1 are in between A1B and IPCC Commitment.

Table 2. Change in cumulative snowmelt depth and total streamflow on 31th May

Under present climatic condition for the ablation period (01st Feb–31st May)			Cumulative snowmelt depth, cm		121.40
			Total streamflow volume, cumec		13.66
Scenarios	Year	Increase in Precipitation (%)	Increase in Temperature (°C)	Increase in cumulative snowmelt depth (cm)	Increase in streamflow volume (%)
A1B	2020	6	0.44	10.98	10.03
	2030	-10	0.84	21.08	-6.26
	2040	18	0.97	24.38	19.87
	2050	-7	1.62	41.11	-2.48
A2	2020	-14	0.27	6.70	-9.98
	2030	-2	0.69	17.28	3.09
	2040	22	0.50	12.50	25.28
	2050	-3	1.18	29.72	0.81
B1	2020	-12	0.30	7.46	-8.10
	2030	-3	0.45	11.24	1.83
	2040	2	0.66	16.53	6.36
	2050	-4	0.58	14.51	1.02
IPCC Commitment	2020	-4	0.25	6.2	0.59
	2030	-2	0.26	6.45	2.89
	2040	3	0.13	3.22	6.19
	2050	7	-0.06	-1.49	5.94

Under IPCC Commitment, instead of shifting in backward direction, depletion ends one day ahead compared to present climatic condition in 2050.

Depletion patterns under different projected scenarios differ from CDC. Using CDC_{CLIM} along with projected temperature and precipitation, streamflows were simulated for different future years under projected climatic scenarios. It can be inferred that for all future years, the A1B climatic scenario affects the snow cover depletion most, as a result, the depletion of snow completes faster in this scenario. Climate affected depletion curve under IPCC Commitment almost matches with CDC for present climate. Climate affected depletion curves under A2 and B1 scenarios are in between A1B and IPCC Commitment.

On a randomly selected date of 26th April, it is found that under present climatic condition, the snow covered extent is 16.41 km^2. In 2020, the extent of SCA is highest under IPCC Commitment (15.80 km^2) followed by A1B (15.49 km^2) scenario. Both A2 and B1 scenarios show the same snow cover extent as 15.18 km^2. In 2030, IPCC Commitment and B1 show least shrinkage having the same snow cover extent as in 2020. A1B scenario has the highest shrinkage (13.89 km^2) followed by A2 (14.86 km^2). But in 2040, the total snow cover extent is increased from 2030 under all projected scenarios except B1. Under IPCC Commitment, the snow cover extent is same as the present condition (16.41 km^2) and the highest decrease in snow cover extent, compared to present condition, is under A1B followed by B1 and A2 scenarios. In 2050, as expected, A1B has the lowest snow extent of 12.51 km^2; followed by A2 with 13.55 km^2; and then B1 having the same snow extent as 2040 (14.86 km^2). However, under IPCC Commitment scenario, the snow cover extent showed an increase from the present snow cover extent by 3.7%. Increase in projected temperature results into increased runoff and reduced SCA due to increase in snowmelt. Therefore, when considering effect of temperature only, it can be said that SCA and projected runoff are inversely related. This is well supported with some exceptions. The exceptions are due to the fact that projected precipitation also affects runoff. Increase in precipitation causes increase in rainfall-induced runoff even if, at the same time, temperature is projected to decrease causing an increase in SCA.

With variations in temperature and precipitation under projected climatic scenarios for future years of 2020, 2030, 2040, and 2050, the cumulative snowmelt depth also varies. It was observed that, the change in the cumulative snowmelt depth followed the same trend as change in temperature with respect to present climatic condition in different future years under all projected scenarios (Table 2). In 2020, the increased temperature is minimal so the melt depth under all projected scenarios closely corresponds to the present climate melt depth. In 2030, as the temperature further increased, the melt depth of all scenarios also increased. Temperature increase is projected to be maximum in A1B; therefore, it has the highest

projected melt depth, followed by A2 and B1 scenarios. But IPCC Commitment affects the least in 2020. In 2040, melt depth under A1B is highest followed by B1 then A2. Melt depths under IPCC Commitment scenario stayed close to present climate in all future years. In 2050, the projected cumulative snowmelt depth under A1B was found highest that crossed 160 cm, followed by A2 in which cumulative melt depth reached 150 cm.

B1 remained closely comparable to cumulative melt depth 137 cm in 2040. In case of IPCC Commitment scenario, the projected temperature decreases in 2050 from present climate and its effect is reflected in cumulative snowmelt depth, which is lesser than the melt depth in present climatic condition. For different future years, it can be said that projected cumulative snowmelt depths are maximum under A1B and minimum under IPCC Commitment. A2 and B1 values are in-between A1B and IPCC Commitment. Under all projected scenarios for different future years, the effects of increased cumulative snowmelt depth are not directly reflected into the projected streamflow. Under A1B and A2 scenarios, the cumulative melt depth is highest in 2050 but it is not reflected in streamflow of 2050. Instead, the streamflow volume in 2050 decreases further from the present climate streamflow volume at the end of snow depletion period. Under B1 scenario, the streamflow is closely corresponding to cumulative snowmelt depth. In 2040 the melt depth is highest, so is the streamflow. And under IPCC Commitment scenario, the effects are opposite as compared to other projected scenarios. In 2050 the cumulative snowmelt depth decreases from the present climate but the streamflow is highest in 2050. IPCC Commitment is the only scenario,which is closely comparable to present climatic condition. From this result, it is apparent that in future years the cumulative snowmelt depth is increasing due to warmer climate and the streamflow volume is decreasing during summer season.

As expected, in different future years under all projected scenarios, the change in cumulative snowmelt depth follows the same trend as change in temperature from present climatic condition. The percentage change in total streamflow from present climatic condition follows almost the same trend as change in precipitation from present climatic condition in different future years under all projected scenarios. But, the percentage change in total streamflow, from present climatic condition does not follow the trends of cumulative snowmelt depth. So, it can be concluded from this study that for eastern Himalayan river basin having seasonal snow cover, the total streamflow under projected climatic scenarios in future years will be primarily governed by the change in precipitation and not by change in snowmelt depth. Among different future years of 2020, 2030, 2040, and 2050, percentage increase in streamflow is maximum in 2040 under all projected scenarios. Among different scenarios, in 2040, increase in streamflow is highest for A2 scenario followed by A1B, B1, and IPCC Commitment. But, increase in precipitation is highest for A2 scenario followed by A1B, IPCC Commitment, and B1. Effect of change in cumulative snow melt depth is visible on change in streamflow, when increase in precipitation is almost same for two future scenarios (e.g., for B1 and IPCC Commitment scenarios in 2040).

CONCLUSIONS

The WinSRM can be recommended to estimate the daily discharge from mountainous basins of eastern Himalaya. Changes in cumulative snowmelt depth for different future years are highest under A1B and lowest under IPCC Commitment. A2 and B1 values are in-between A1B and IPCC Commitment. Advancing of depletion curves for different future years are highest under A1B and lowest under IPCC Commitment. A2 and B1 values are in-between A1B and IPCC Commitment. For the present river basin having seasonal snow cover, the total stream flow under projected climatic scenarios in future years will be primarily governed by the change in precipitation.

ACKNOWLEDGEMENT

The authors gratefully acknowledge the encouragement and financial support provided by Department of Science and Technology, Technology Bhawan, New Mehrauli Road, New Delhi. The authors express their sincere thanks to WRD (Itanagar) for extending help and logistic support, and CWC and NRSC for providing the data for use in this study. Special thanks are due to Snow and Avalanche Study Establishment, Defence Research and Development Organisation, Him Parisar, Chandigarh for installing the AWS at study site, and to the Indian Army for providing space and security to the AWS.

REFERENCES

Bandyopadhyay, A., Bhadra, A., Maza, M. Shelina, R.K. 2014. Monthly Variations of Air Temperature Lapse Rates in Arunachal Himalaya. Journal of Indian Water Resources Society, v.34(3), pp:16-25. ISSN: 0970-6984.

Bates, B.C., Kundzewicz, Z.W., Wu, S. and Palutikof, J.P. (Eds.) 2008. Climate change and water. Technical paper of the Intergovernmental Panel on Climate Change, IPCC Secretariat, Geneva.

Collins, W.D., Bitz, C.M., Blackmon, M.L., Bonan, G.B., Bretherton, C.S., Carton, J.A., Chang, P., Doney, S.C., Hack, J.J., Henderson, T.B., Kiehl, J.T., Large, W.G., McKenna, D.S., Santer, B.D. and Smith, R.D. 2006. The community climate system model version 3 (CCSM3). Journal of Climate, v.19, pp:2122-2143.

Girod, B., Wiek, A., Mieg, H. and Hulme, M. 2009. The evolution of the IPCC's emissions scenarios. Environmental Science & Policy, doi:10.1016/j.envsci. 2008.12.006.

Hughes, D.A., Hannart, P. and Watkins, D. 2003. Continuous baseflow separation from time series of daily and monthly streamflow data. Water SA, v.29(1), pp:43-48.

Kulkarni, A.V., Singh, S.K., Mathur, P. and Mishra, V.D. 2006. Algorithm to monitor snow cover using AWiFS data of RESOURCESAT-1 for the Himalayan region. International Journal of Remote Sensing, v.27(12), pp:2449-2457.

Kulkarni, A.V., Srinivasulu, J., Manjul, S.S. and Mathur, P. 2002. Field based spectral reflectance studies to develop NDSI method for snow cover monitoring. Journal of the Indian Society of Remote Sensing, v.30(1&2), pp:73-80.

Martinec, J. 1960. The degree-day factor for snowmelt runoff forecasting. IAHS Publ. v.51, pp:468-477.

Martinec, J., Rango, A. and Roberts, R. 2008. Snowmelt runoff model (SRM)-User's manual. WinSRM version 1.11. Edited by Gomez-Landesa, E. and Bleiweiss, M.P., New Mexico State University, Las Cruces, New Mexico, USA.

Nakicenovic, N., Grubler, A., Gaffin, S., Jung, T.T., Kram, T., Morita, T., Pitcher, H., Riahi, K., Schlesinger, M., Shukla, P.R., Vuuren, D.Y., Davis, G., Michaelis, L., Swart, R. and Victor, N. 2003. IPCC SRES Revisited: A Response. Energy & Environment, v.14(2&3), pp:187-214.

Pachauri, R.K. and Reisinger, A. (Eds.) 2007. Climate change (AR4): Synthesis report. Contribution of working groups I, II and III to the fourth assessment report of the Intergovernmental Panel on Climate Change (IPCC), Geneva, Switzerland.

Rango, A. and Martinec, J. 1994. Model accuracy in snowmelt-runoff forecasts extending from one to 20 days. Water Resources Bulletin, v.30(3), pp:463-470.

Singh, P. and Jain, S.K. 2002. Snow and glacier melt in the Satluj river at Bhakra Dam in the western Himalayan region. Hydrological Sciences Journal, v.47(1), pp:93-106.

Singh, P. and Kumar, N. 1997. Impact assessment of climate change on the hydrological response of a snow and glacier melt runoff dominated Himalayan river. Journal of Hydrology, 193(1-4), pp:316-350.

Singh, P. and Singh, V.P. 2001. Snow and glacier hydrology. Kluwer Academic publishers, Dordrecht, The Netherlands

Swain, E., Stefanova, L. and Smith, T. 2014. Applying downscaled global climate model data to a hydrodynamic surface-water and groundwater model. American Journal of Climate Change, v.3, pp:33-49.

Welderufael, W.A. and Woyessa, Y.E. 2010. Stream flow analysis and comparison of base flow separion methods – Case study of the Modder river basin in central south Africa. European Water, v.31, pp:3-12.

WMO 1964. Guide for hydrometeorological practices. World Meteorological Organisation (WMO), Geneva, Switzerland.

WMO 1986. Intercomparison of models of snowmelt runoff. Operational Hydrology Report no. 23, World Meteorological Organisation (WMO) no. 646, Geneva.

WMO 1992. Simulated real-time intercomparison of hydrological models. World Meteorological Organisation (WMO) Operational Hydrology Report no. 38, WMO no. 779, Geneva.

Dr. Arnab Bandyopadhyay is currently working as Associate Professor in Department of Agricultural Engineering, NERIST, Arunachal Pradesh. His areas of interest are Surface Hydrology, Mathematical Modeling, RS and GIS Application in Water Resources, and Vulnerability to Climate Change. He is Life Members of Indian Society for Technical Education, Indian Association of Hydrologists, Indian Water Resources Society, and Indian Society of Remote Sensing. Earlier he worked as Scientist in National Institute of Hydrology.

Dr. Aditi Bhadra is working as Associate Professor in Department of Agricultural Engineering, NERIST, Arunachal Pradesh. Her areas of interest are Hydrological Modelling, Operation and Management of Reservoir-based Canal Irrigation Projects, Snow Hydrology, and Soil and Water Engineering. She is the recipient of Indo-US Research Fellowship 2012 for PostDoc Research at UC Merced. She is an Associate Member of Institute of Engineers (India) and Life Members of Indian Assoc. of Soil and Water Conservationists and Soil Conservation Society of India.

Mr. Ngahorza Chiphang is currently working as an SRF in the Department of Agricultural Engineering, NERIST, Arunachal Pradesh. He is developing a raster-based snowmelt runoff modelling system.

Dr. Kshetrimayum Tayal Senzeba has completed his Ph.D. in snow hydrology in 2015. He is currently working as a Subject Matter Specialist in ICAR.